Molecular Therapy
Nucleic Acids
Original Article

Human Amniotic Epithelial Cell-Derived Exosomes Restore Ovarian Function by Transferring MicroRNAs against Apoptosis

Qiuwan Zhang,[1,2,3] Junyan Sun,[1] Yating Huang,[1] Shixia Bu,[1] Ying Guo,[1] Tingting Gu,[1] Boning Li,[1] Chunhui Wang,[4] and Dongmei Lai[1,2,3]

[1]The International Peace Maternity and Child Health Hospital, School of Medicine, Shanghai Jiao Tong University, Shanghai 200030, China; [2]Shanghai Key Laboratory of Embryo Original Diseases, Shanghai 200030, China; [3]Shanghai Municipal Key Clinical Speciality, Shanghai 20030, China; [4]Shanghai iCELL Biotechnology Co., Ltd., Shanghai 200333, China

Premature ovarian failure (POF) is one of the most common complications among female patients with tumors treated with chemotherapy and requires advanced treatment strategies. Human amniotic epithelial cell (hAEC)-based therapy mediates tissue regeneration in a variety of diseases, and increasing evidence suggests that the therapeutic efficacy of hAECs mainly depends on paracrine action. This study aimed to identify exosomes derived from hAECs and explored the therapeutic potential in ovaries damaged by chemotherapy and the underlying molecular mechanism. hAEC-derived exosomes exhibited a cup- or sphere-shaped morphology with a mean diameter of 100 nm and were positive for Alix, CD63, and CD9. hAEC exosomes increased the number of follicles and improved ovarian function in POF mice. During the early stage of transplantation, hAEC exosomes significantly inhibited granulosa cell apoptosis, protected the ovarian vasculature from damage, and were involved in maintaining the number of primordial follicles in the injured ovaries. Enriched microRNAs (miRNAs) existed in hAEC exosomes, and target genes were enriched in phosphatidylinositol signaling and apoptosis pathways. Studies *in vitro* demonstrated that hAEC exosomes inhibited chemotherapy-induced granulosa cell apoptosis via transferring functional miRNAs, such as miR-1246. Our findings demonstrate that hAEC-derived exosomes have the potential to restore ovarian function in chemotherapy-induced POF mice by transferring miRNAs.

INTRODUCTION

Premature ovarian failure (POF) is defined as the cessation of ovarian function before the age of 40 years, accompanied with amenorrhea, hypergonadotropic hypogonadism, and infertility.[1,2] The most important and common cause of POF is chemotherapy used to treat female cancer patients.[2] The ovarian reserve depends on the number of quiescent follicles in ovaries, and the activation of dormant follicles is mediated by the phosphatidylinositol 3-kinase (PI3K)/Akt signaling pathway.[3] Research demonstrated that chemotherapy agents, such as cyclophosphamide and busulfan *in vivo* experiment (Cy) trigger the growth of the quiescent primordial follicle by upregulating PI3K/Akt signaling, resulting in the loss of the ovarian reserve, which occurs simultaneously with granulosa cell apoptosis.[4] Therefore, exploring new strategies for preserving the ovarian reserve and preventing infertility has become an urgent need.

With the development of regenerative medicine, stem cell-based transplantation is a promising strategy for restoring ovarian function and reversing fertility in female mice and POF patients.[5–7] Accumulating evidence suggests that bone marrow stem cell (BMSC) transplantation rescues fertility and repairs ovarian function by promoting ovarian angiogenesis,[8] the transplantation of umbilical cord MSCs (UC-MSCs) on a collagen scaffold activates dormant follicles in patients with a long history of infertility,[6] and human chorionic plate-derived MSCs restore ovarian function in chemotherapy-induced POF mice.[9] However, stem-cell-based therapies still face several challenges, including transplant rejection, tumor transformation, limited sources, and ethical problems associated with clinical application. As an alternative, the discarded placenta offers an extraordinary source of fetal stem cells, such as human amniotic epithelial cells (hAECs), which retain the characteristics of embryonic stem cells, including immunomodulation, anti-inflammatory properties, and low immunogenicity.[10] Because of these advantageous characteristics, hAECs have been widely used in regenerative medicine and have obtained a good outcome after transplantation in many diseases, including lung injury,[11] brain injury,[12,13] and hepatic fibrosis.[14]

Because stem cell transplantation is hampered by the poor survival of the implanted cells, studies have increasingly focused on the paracrine action of stem cells. In previous studies, we have elucidated that only a small quantity of transplanted hAECs directly differentiate into

Received 3 December 2018; accepted 16 March 2019;
https://doi.org/10.1016/j.omtn.2019.03.008.

Correspondence: Dongmei Lai, MD, PhD, The International Peace Maternity and Child Health Hospital, School of Medicine, Shanghai Jiao Tong University, Shanghai 200030, China.
E-mail: laidongmei@hotmail.com

granulosa cells in chemotherapy-induced POF mice.[15] More important, hAEC-derived conditioned medium (hAEC-CM) has the potential to restore ovarian function by attenuating apoptosis,[16] enhancing angiogenesis,[17] and promoting follicular development.[18] Meanwhile, studies have reported that hAEC-CM rescues cell death through directly mediating brain immune cells following injury,[19] and hAEC-derived soluble factors suppress collagen production and reduce proliferation in human hepatic stellate cells.[20] Thus, the paracrine pathway plays an important role in the process of hAEC-mediated tissue functional recovery.

Exosomes are a family of nanoparticles with a diameter in the range of 40–150 nm produced by multivesicular bodies and carry bioactive cytokines, growth factors, signaling lipids, mRNAs, long noncoding RNAs (lncRNAs), and regulatory microRNAs (miRNAs).[21,22] One of the most attractive features is that exosomes can regulate cellular function via transferring cargo into recipient cells.[23] Accumulating studies have demonstrated that the transplantation of these nanoparticles has pro-regenerative effects in injured tissues and avoids many risks associated with stem cell transplantation therapy.[24,25] Recent studies have reported that hAEC-derived exosomes restrict lung injury and enhance endogenous lung repair in bleomycin-challenged aged mice,[26] accelerate wound healing, and inhibit scar formation.[27] Therefore, the paracrine action of hAECs can be partially attributed to exosomes, and the exploitation of hAEC exosomes as a therapy for POF should be interesting and meaningful.

In the current study, we mainly focused on identifying exosomes derived from hAECs and investigated the effect of hAEC exosomes on follicle development and ovarian function in chemotherapy-induced POF mice. Furthermore, granulosa cells and ovarian vascular were observed in the early stage of hAEC exosome transplantation. Finally, we analyzed the miRNA profiles of hAEC exosomes and further explored the underlying molecular mechanism in the process of hAEC-exosome-inhibited granulosa cell apoptosis *in vitro*.

RESULTS

The Enrichment of Exosomes Existed in hAEC-CM

The isolated hAECs exhibited a cobblestone-like morphology under a microscope (Figures 1A and 1a) and expressed a high level of the stem cell marker SSEA4 (99.6%) and the epithelial marker CD324 (99.4%), as shown in Figure 1B.

hAECs were cultured in complete medium without bovine serum for 24 h, and exosomes were isolated from the hAEC-CM, as shown in Figure 1F. The morphological assessment revealed the typical cup-shaped morphology of exosomes with an approximately 100 nm diameter, as determined by transmission electron microscopy (Figure 1C). Western blot results showed the presence of exosomal markers, including Alix, CD63, and CD9 in the hAEC exosomes. Furthermore, the expression of exosomal markers was significantly inhibited when hAECs were pre-treated with 10 μM GW4869, a selective inhibitor of N-SMase (Figure 1D). To further analyze the size distribution of the hAEC-derived exosomes, we performed size analysis, using a nanoparticle tracking system with a peak size of 50–150 nm (Figure 1E). The hAEC-derived exosomes were highly enriched in the CM and could be successfully harvested for the further POF animal experiments, as shown in Figure 1F.

hAEC-Exosome Transplantation Restored Ovarian Function in Chemotherapy-Treated Mice

In previous studies, we reported that paracrine action of hAECs plays a vital role in the process of restoring ovarian function.[18] To investigate the long-term function of hAEC-derived exosomes on ovarian function, we established different treatments groups, including PBS, hAEC exosomes, hAEC-CM, and hAEC-CM without exosomes [hAEC-CM (GW4869)], in which hAECs were pre-treated with GW4869. Transplantation was conducted at 1 week (orthotopic injection$^{9th\ week}$) and 2 weeks (tail vein injection$^{10th\ week}$) after chemotherapy. The follicle development and ovarian function were evaluated at 4 weeks after the treatments.

In the Sham (untreated control) group, the ovaries contained numerous healthy follicles at different stages. In contrast, mice in the PBS-treated chemotherapy group showed atrophied ovaries composed of interstitial cells in a fibrous matrix. In addition, chemoablated mice demonstrated that a statistically significant reduction in the number of primordial, primary, secondary, and mature follicles (Figures 2A and 2B; $p < 0.05$). Interestingly, a few healthy mature follicles were observed in the injured ovaries of mice injected with hAEC exosomes, hAEC-CM, and hAEC-CM (GW4869) (Figure 2A). According to the results of the follicle count, both hAEC exosomes and hAEC-CM transplantation significantly increased the number of mature follicles compared with that observed following the PBS injection in chemotherapy-treated mice. Importantly, the number of primordial and primary follicles in the hAEC-exosome transplantation group was higher than those in the PBS-treated chemotherapy control group (Figure 2B; $p < 0.05$). Additionally, ovaries were subjected to mRNA array analysis to systematically assess the difference in ovarian function between the hAEC-exosome and PBS-treated groups. The Kyoto Encyclopedia of Genes and Genomes (KEGG) and Gene Ontology (GO) analyses showed that hAEC-exosome transplantation reversed the decreased biological process induced by chemotherapy, including brown fat cell differentiation, the lipid catabolic process, the metabolic pathways, proliferator-activated receptor gamma (PPARγ), and the AMP-activated protein kinase (AMPK) signaling pathways, while simultaneously decreasing biological processes, including cellular response to interleukin-1 and tumor necrosis factor in the ovaries of the POF mice (Figure 2C). These results indicate that hAEC exosomes have the potential to repair ovarian function in a POF mouse model.

hAEC Exosomes Inhibited Granulosa Cell Apoptosis and Attenuated the Acute Vascular Injury Induced by Chemotherapy in Mouse Ovaries

A previous study[4] demonstrated that granulosa cell apoptosis in growing follicles and acute vascular injury were prominent characteristics of chemotherapy drugs leading to reduced fertility.[4] To further

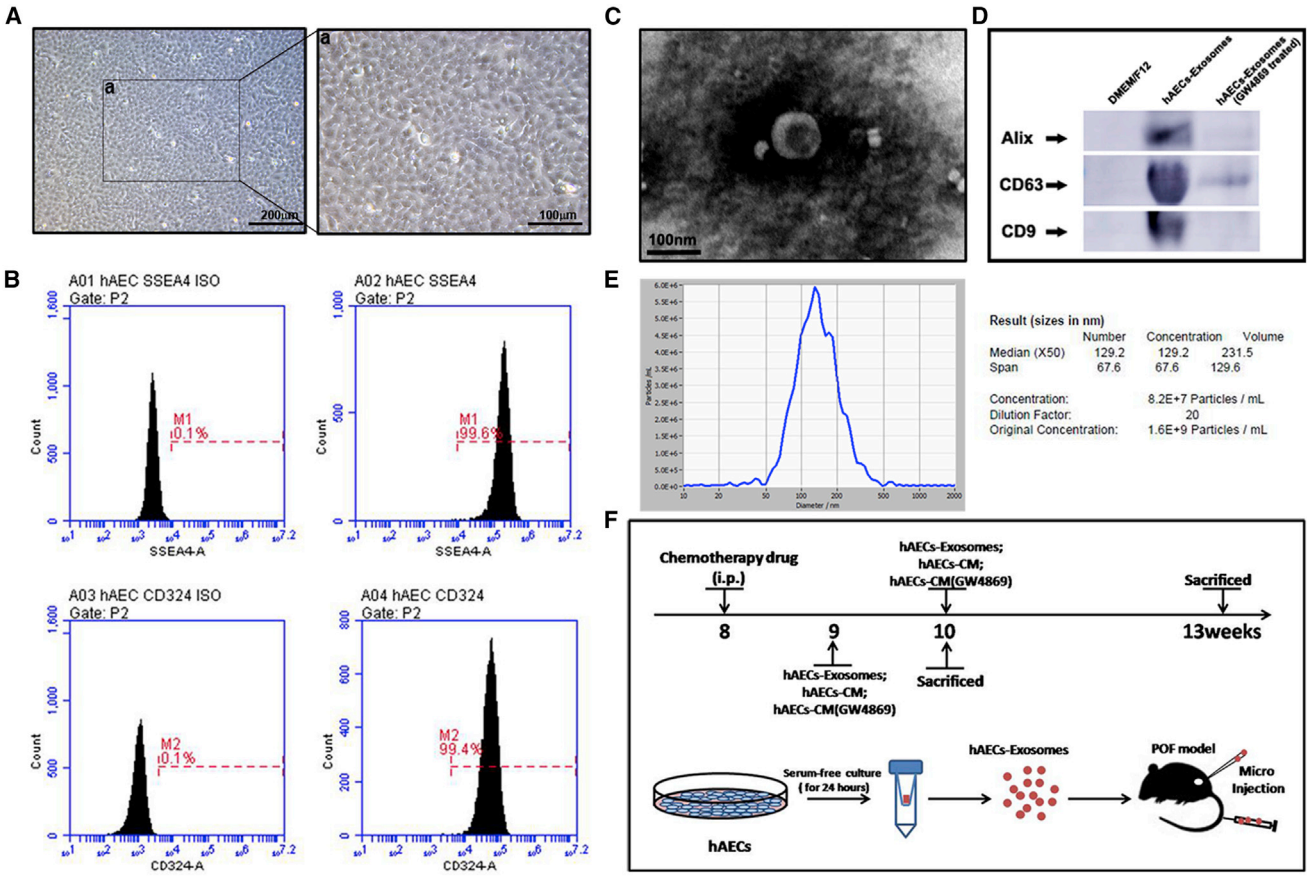

Figure 1. Characterization of Exosomes Derived from hAEC-Conditioned Medium and the Design of Animal Experiments

(A) The morphology of hAECs was observed under a microscope. Scale bar, 200 μm in (A) and 100 μm in (a). (B) Flow cytometry analysis of cell surface markers on hAECs. The isotypes (ISO) of SSEA4 and CD324 were used as negative controls. (C) Morphology of hAEC exosomes under transmission electron microscopy. Scale bar, 100 nm. (D) Western blot was used to detect the expression of the exosomal markers Alix, CD63, and CD9 in hAEC-derived exosomes. (E) The mean diameter of hAEC exosomes was analyzed using a nanoparticle tracking system (NTA). Approximately 1.6×10^9 particles were measured by NTA in hAEC exosomes (in a single injection), which came from a total of 5×10^6 hAECs. (F) Schematic of the experimental procedure was used to harvest exosomes from the hAEC-conditioned medium and showed the animal experimental design.

investigate the effect of hAEC exosomes on granulosa cell function and ovarian vascular, mice were injected intraperitoneally with 5-ethynyl-2′-deoxyuridine (EdU) 24 h prior to sacrifice. The ovarian morphology was observed at 1 week after hAEC-exosome transplantation.

Results showed that a large number of EdU-positive cells were observed in granulosa cells of growing follicles in the Sham group. However, the proliferation of granulosa cells was significantly inhibited in the PBS-treated chemotherapy group. Although hAEC-exosome transplantation did not increase granulosa cell proliferation, it inhibited the acute vascular injury induced by chemotherapy (Figures 3A and 3B; $p < 0.05$). A few mature follicles were observed in the ovaries of the PBS-treated chemotherapy group, in which granulosa cells of cumulus oocyte complexes (COCs) were in disorder and positive for terminal deoxynucleotidyl transferase mediated dUTP nick end labeling (TUNEL) staining, as indicated by the white arrowhead (Figure 3C). However, hAEC exosomes significantly inhibited chemotherapy-induced apoptosis of cumulus granulosa cells (Figure 3C). Cumulus granulosa cells play a vital role in the regulation of COC functions by producing hyaluronic acid. Our results showed that chemotherapy significantly decreased the expression of cumulus expansion-related genes, including hyaluronic acid synthase 2 (*HAS2*) and pentraxin 3 (*PTX3*); however, hAEC-exosome transplantation upregulated *HAS2* expression (Figure 3D; $p < 0.05$). Consistent with the morphological results, hAEC-exosome transplantation effectively reversed the increased cleaved Caspase 3 induced by chemotherapy (Figure 3E; $p < 0.05$). These results demonstrate that hAEC-derived exosomes protect follicular development by attenuating acute vascular damage and inhibiting granulosa cell apoptosis in the early stage of transplantation.

hAEC Exosomes Partially Prevented Primordial Follicle Activation in Chemotherapy-Treated Mice

A previous study demonstrated that granulosa cell apoptosis was a causative factor accelerating follicular depletion and atresia

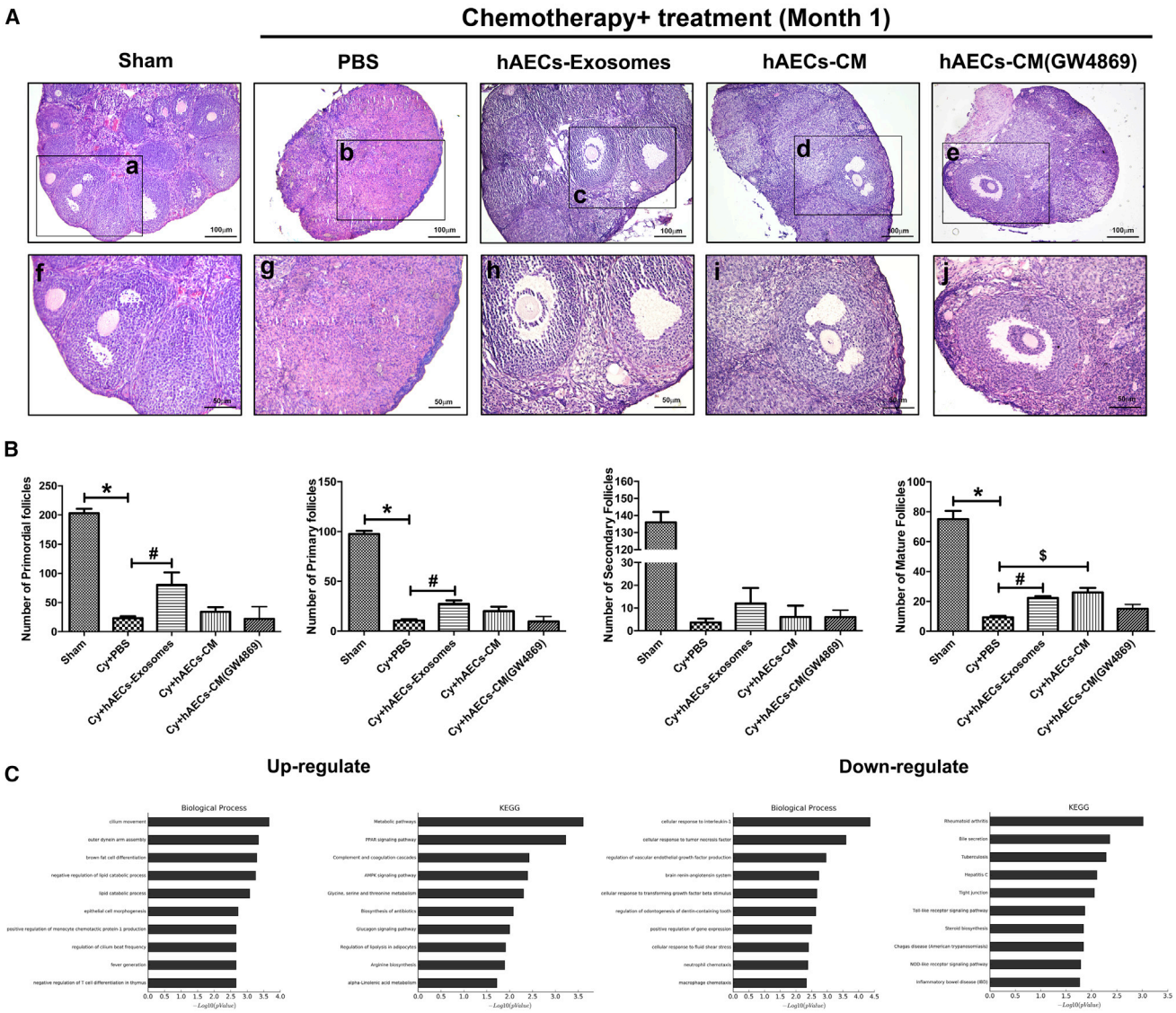

Figure 2. Effect of hAEC Exosomes on Follicle Development and Ovarian Function in Chemotherapy-Treated Mice

(A) Representative photomicrographs of H&E-stained ovarian sections in different groups. Images f, g, h, i, and j are magnifications of the squares in images a, b, c, d, and e, respectively. Scale bar, 100 (top) and 50 (bottom) μm. (B) The columns display the number of primordial, primary, secondary, and mature follicles per ovary in the different treatment groups. (C) Bioinformatics analysis of the differential gene expression in injured ovaries between the PBS and hAEC-exosome-treated groups. The data represent means ± SEM. Sham group, n = 6; Cy+PBS group, n = 6; Cy+hAEC exosome group, n = 6; Cy+hAECs-CM group, n = 6; and Gy+hAECs-CM (GW4869) group, n = 6. *$p < 0.05$ versus Sham group; #$p < 0.05$ versus Cy+PBS group; $$p < 0.05$ versus Cy+PBS group.

depending on the PI3K/Akt/mTOR pathway, which was also negatively regulated by follicle development. In the present study, we examined whether hAEC-exosome transplantation affects the process of primordial follicle activation induced by chemotherapy. The morphology of ovarian sections showed that the number of primordial, primary, secondary, and mature follicles was significantly decreased in PBS-treated mice in the chemotherapy group compared with the Sham group. However, hAEC-exosome transplantation significantly increased the number of primordial follicles and mature follicles in the injured ovaries compared with those in the PBS-treated chemotherapy group (Figures 4A and 4B; $p < 0.05$). Because the activation of primordial follicles depends on the PI3K/Akt/mTOR pathway, we detected the expression of related proteins in the different treatment groups. Western blot results showed that chemotherapy significantly increased p-Akt, p-mTOR, and p-FoxO3a protein expression in ovaries. However, hAEC exosomes slightly reduced p-Akt and p-FoxO3a expression in injured ovaries (Figure 4C and 4D; $p < 0.05$). These results

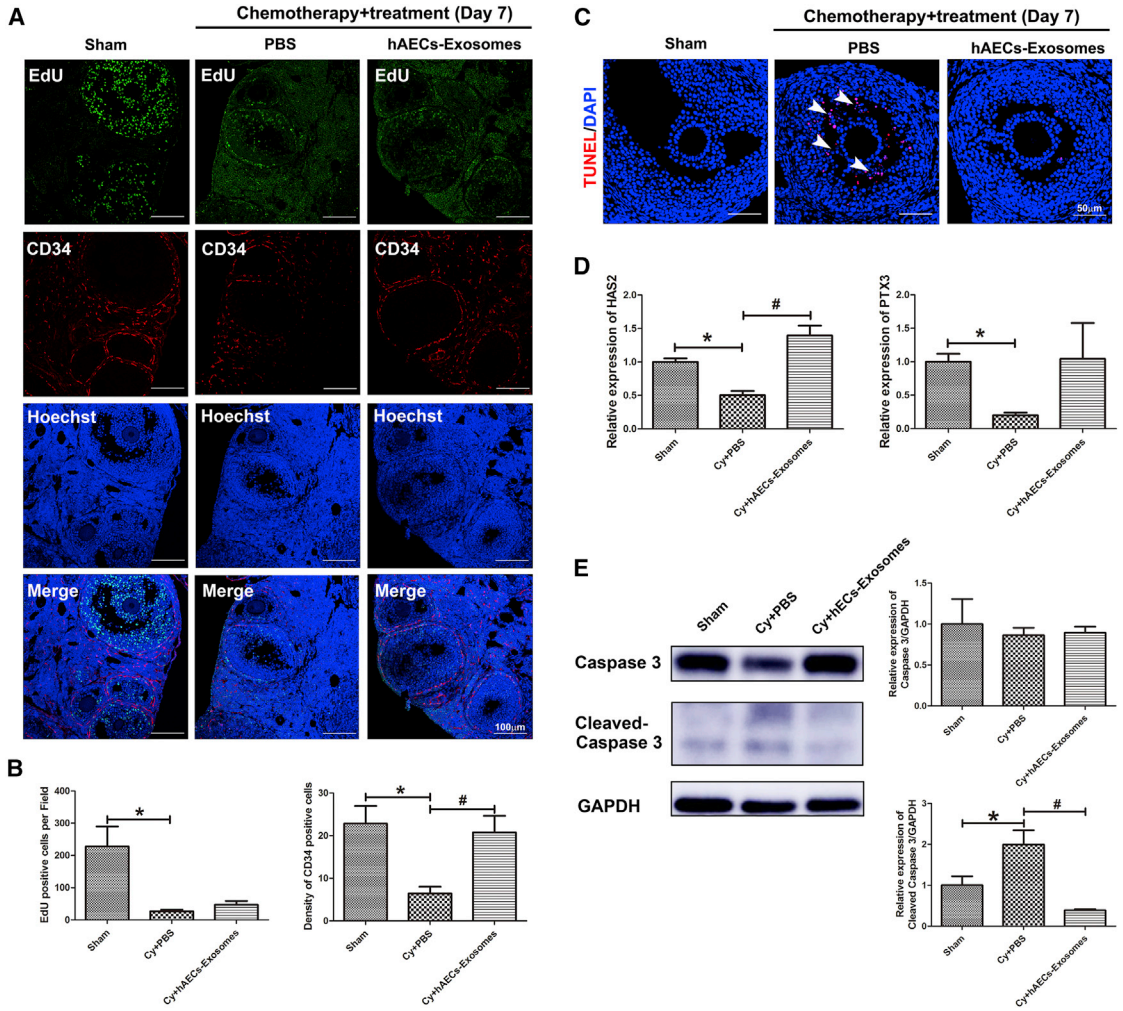

Figure 3. Effect of hAEC Exosomes on Ovarian Vasculature and Granulosa Cells Function in Chemotherapy-Treated Mice

(A) Double immunofluorescence of EdU and CD34 in ovarian sections. Scale bar, 100 μm. (B) The columns show the number of EdU- and CD34-positive cells among the different treatment groups. (C) TUNEL staining was used to detect the granulosa cell apoptosis induced by chemotherapy. Scale bar, 50 μm. (D) qRT-PCR was performed to detect the expression of the cumulus expansion genes *HAS2* and *PTX3* in the different groups. (E) Western blot was conducted to detect the expression of cleaved Caspase 3 in the injured ovaries. The data represent means ± SEM. Sham group, n = 6; Cy+PBS group, n = 6; Cy+hAEC-exosome group, n = 6. *p < 0.05 versus Sham group; #p < 0.05 versus Cy+PBS group.

revealed that hAEC exosomes partially inhibited the primordial follicle activation induced by chemotherapy.

MicroRNA Expression Profiles of hAEC Exosomes and Target Gene Pathway Enrichment Analysis

To obtain a better understanding of how hAEC exosomes regulate ovarian function, we used a miRNA array and bioinformatics to analyze the miRNA landscape of hAEC-derived exosomes. Five exosome samples were harvested from different donor-derived hAECs. miRNAs in hAEC exosomes were profiled by Nanostring and rank ordered according to total reads from highest to lowest, normalized to positive controls, and the top 50 miRNAs are shown from highest to lowest (Figure 5A). The top 30 miRNA target genes were analyzed to identify statistically over-represented pathways and biological processes. The majority of the genes substantially contributed to the specific processes related to the phosphatidylinositol signaling system, PPAR signaling pathway, and apoptotic process involved in morphogenesis (Figures 5B and 5C). Meanwhile, the network of miRNAs was predicted to target mainly the genes that control processes related to the PI3K pathway, as shown in Figure 5D. qRT-PCR results also verified that hsa-miR-1246 was highly expressed in exosomes derived from hAECs (Figure 5E).

hAEC Exosomes Inhibited Granulosa Cell Apoptosis Induced by Chemotherapy by Transferring Functional miRNAs

Granulosa cells are important component of follicles that are easily susceptible to chemotherapy-induced damage. Herein, a human ovarian granulosa tumor-derived cell line (KGN cells) was used in

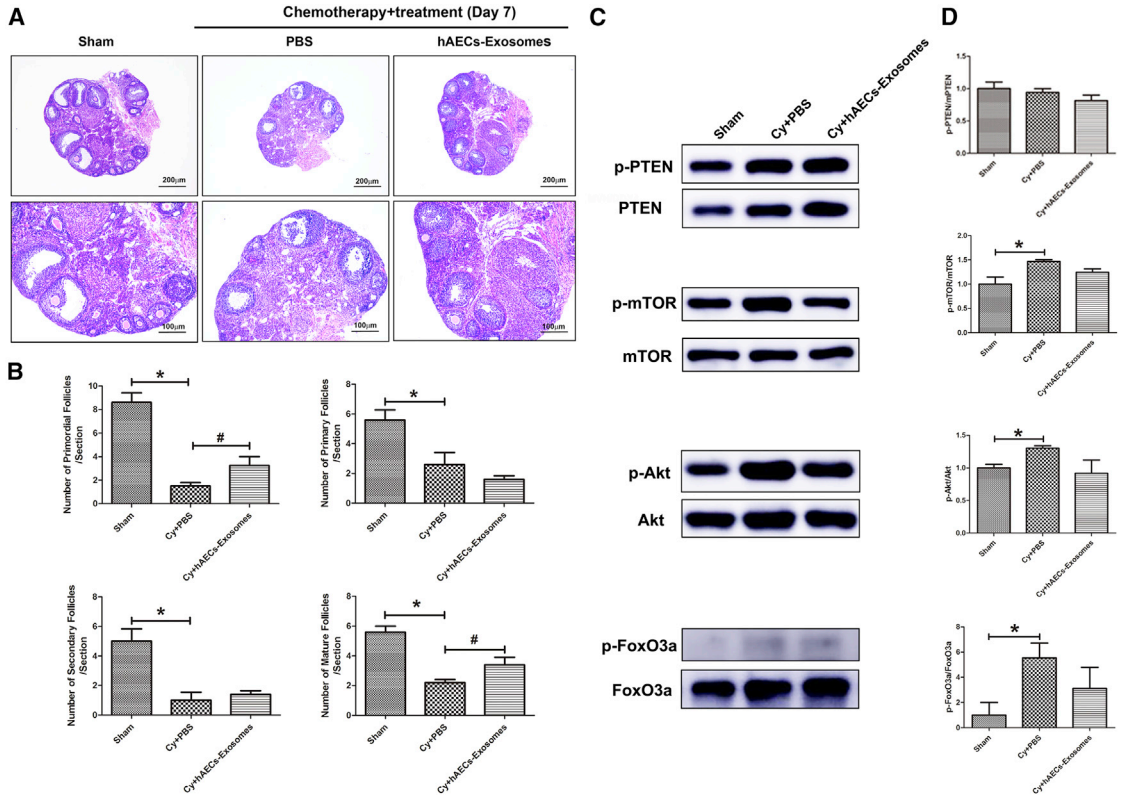

Figure 4. Effect of hAEC Exosomes on Follicular Activation in Ovaries of Chemotherapy-Treated Mice

(A) H&E staining showed the morphology of follicles in the different treatment groups 7 days after transplantation. Scale bars, 200 (top) and 100 (bottom) μm. (B) Columns display the number of primordial, primary, secondary, and mature follicles per ovarian section in the different groups. (C) Western blot was used to detect the expression of PI3K/Akt/mTOR pathway-related proteins in injured ovaries among the different treatment groups. (D) Column showing that hAECs-exosomes partially inhibited the primordial follicle activation induced by chemotherapy. The data represent means ± SEM. Sham group, n = 6; Cy+PBS group, n = 6; Cy+hAEC-exosome group, n = 6. *p < 0.05 versus Sham group.

our experiments. To investigate how hAEC-derived exosomes affect granulosa cells function *in vitro*, we first examined whether hAEC exosomes could be transferred into recipient KGN cells. hAECs were labeled with PKH26 membrane fluorescent dye to perform the tracking experiment. Red fluorescence signaling was observed in the cytoplasm of hAECs 24 h after labeling with PKH26. Then, we collected the CM of PKH26-labeled hAECs, extracted PKH26-labeled exosomes, and added them into the medium of KGN cells (Figure 6A). After 24 h, the fluorescence signal of PKH26-labeled exosomes was observed in the cytoplasm of granulosa cells treated with or without cyclophosphamide treatment *in vitro* experiment (CTX) (Figure 6B). Next, we determined the impact of hAEC exosomes on chemotherapy-induced apoptosis in granulosa cells. As shown in Figure 6C, CTX markedly increased the expression of cleaved Caspase 3, and inhibited the expression of proliferating cell nuclear antigen (PCNA) in granulosa cells. Although hAEC-derived exosomes had no effect on the proliferation of granulosa cells, they significantly inhibited chemotherapy-induced granulosa cell apoptosis, including increasing the expression of the anti-apoptosis genes Bad and Bcl2 and decreasing Bax and cleaved Caspase 3 expression in KGN cells (Figure 6C; $p < 0.05$). qRT-PCR results showed that hAEC exosomes slightly increased miR-1246 expression in granulosa cells (Figure 6D).

Previous research reported that overexpression of miR-21 in stem cells improved ovarian structure and function in chemotherapy-induced ovarian damage by inhibiting granulosa cell apoptosis.[28] To verify whether miR-1246 has a similar function in inhibiting apoptosis, we transfected granulosa cells with miR-1246, miR-21-5p mimic, and scrambled control oligonucleotide. qRT-PCR showed that miR-1246 and miR-21-5p gene expression was dramatically increased in granulosa cells (Figure 6E; $p < 0.05$). Western blot results showed that miR-1246 and miR-21-5p overexpression significantly reversed the increased expression of cleaved Caspase 3 protein induced by chemotherapy in granulosa cells (Figure 6F; $p < 0.05$). Taken together, these results reveal that hAEC-derived exosomes could be transferred into granulosa cells, and inhibit granulosa cell apoptosis via transferring miRNAs.

DISCUSSION

Previous studies[10,20] have demonstrated that hAECs are an excellent source of seed stem cells, which may be used in regenerative therapies

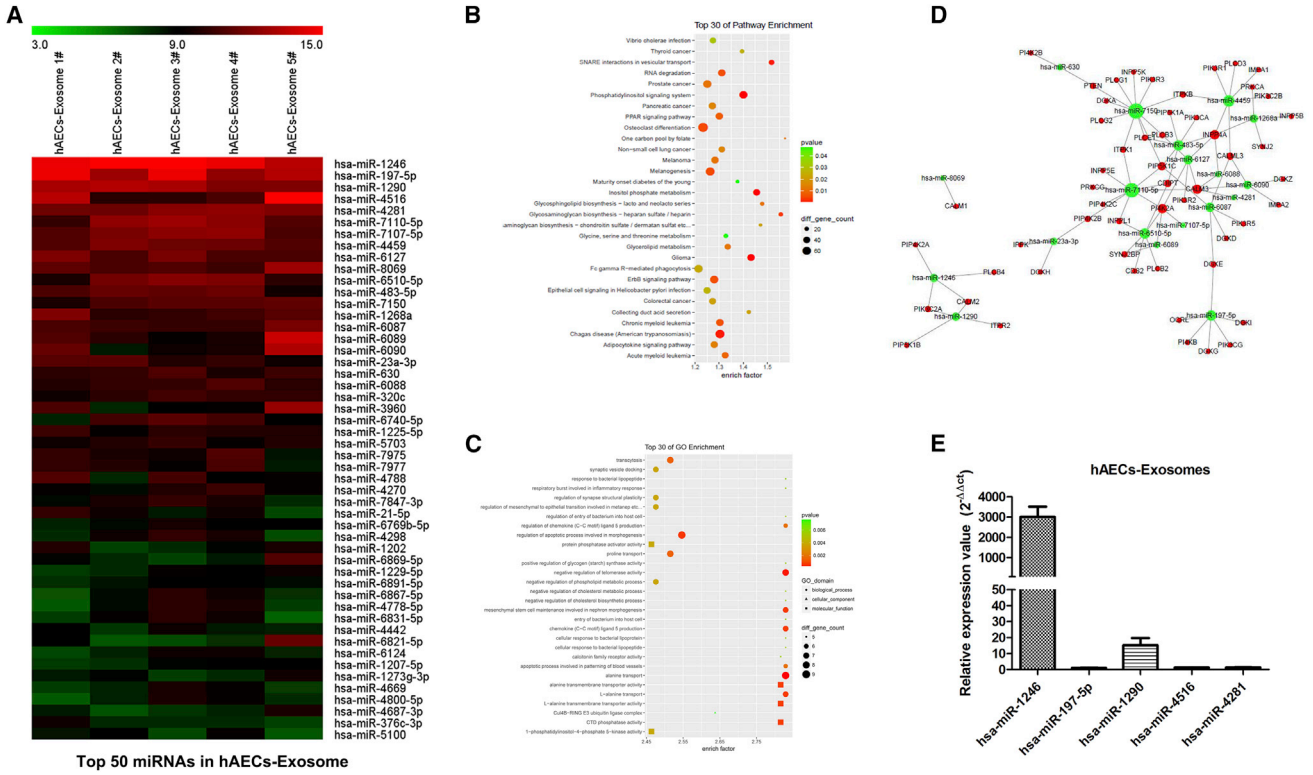

Figure 5. MicroRNA Profile of hAEC Exosomes and Target Gene Pathway Enrichment Analysis

(A) miRNA expression of hAEC exosomes from five biological replicate samples was detected and analyzed by microRNA array. Enrichment pathway (B) and Gene Ontology enrichment (C) targeted by the top 30 miRNAs in hAEC-exosomes. (D) Enrichment map of the phosphatidylinositol 3-kinase signaling pathway targeted by the top 30 miRNAs. (E) qRT-PCR was used to detect miRNA expression in hAEC-derived exosomes.

for a variety of diseases, and the paracrine potential of hAECs has been proven in many animal studies. The present study was the first to report that hAEC exosomes exhibit a therapeutic effect similar to the paracrine action of hAECs in chemotherapy-induced POF mice. hAEC-exosome transplantation not only protected follicles from chemotherapy-induced ovary damage but also repaired ovarian function of POF mice, including enhancing metabolic pathways, PPAR signaling pathways, and AMPK signaling pathways. A previous study demonstrated that PPARγ and AMPK signaling pathways play a role in energy control and lipid metabolism. In mice, the absence of PPAR in ovaries results in lower levels of fertility.[29]

Chemotherapy drugs given to female cancer patients invariably lead to ovarian damage, including granulosa cell apoptosis, ovarian vascular damage, and rapid depletion of the follicle reserve, resulting in POF.[2] Within the ovary, oocytes are stored in the form of primordial follicles, surrounded by somatic granulosa cells. Research demonstrated that chemotherapy treatment led to the hyperactivation of PI3K signaling pathway in ovaries, which was related to the primordial follicle loss and granulosa cell apoptosis. Thus, the global activation of the primordial follicle pool leads to the exhaustion of the remaining follicle reserve.[30] The PI3K/Akt/mTOR cell signaling pathway has been known to regulate the primordial-to-primary transition in mammalian follicle development.[31] Investigating new methods of preventing chemotherapy-induced primordial follicle activation could provide significant advantages over existing fertility-preservation techniques.[32] Research has demonstrated that melatonin prevents cisplatin-induced primordial follicle loss by preventing the phosphorylation of PTEN/Akt/FOXO3a pathway members in POF mice.[33] Furthermore, rapamycin prevents the primordial follicle activation induced by CTX through the PI3K/Akt/mTOR signaling pathway and thus plays a role in preserving the follicle pool.[34] In the current study, we found that hAEC-derived exosomes had the potential to inhibit the granulosa cell apoptosis induced by chemotherapy and to protect the ovarian vasculature from damage. In addition, the hAEC exosomes partially inhibited primordial follicle activation in the early stage of transplantation.

Recently, many studies[24,25,35] have reported that exosome-carrying miRNAs play a crucial role in stem cell-mediated tissue functional repair. The overexpression of miR-21 in stem cells improved ovarian structure and function in rats with chemotherapy-induced ovarian damage by targeting *PDCD4* and *PTEN*, to inhibit granulosa cell apoptosis.[28] In addition, exosomal microRNA-21-5p mediates mesenchymal stem cell paracrine effects on human cardiac tissue

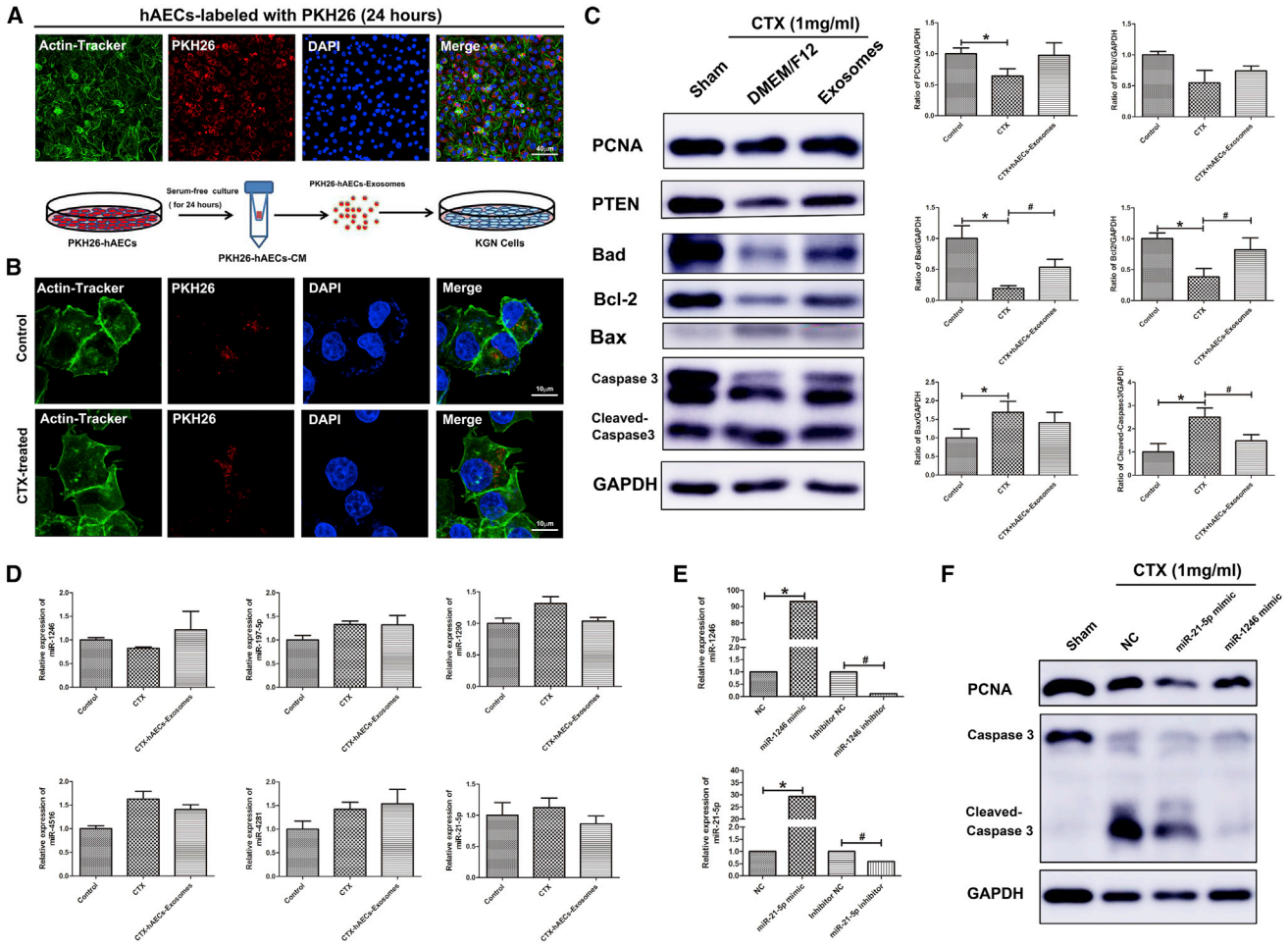

Figure 6. Effect of hAEC-Derived Exosomes on Chemotherapy-Induced Granulosa Cell Apoptosis *In Vitro*

(A) hAECs were labeled with PKH26 fluorescent dye. Schematic of the experimental procedure used to harvest PKH26-labeled exosomes from the PKH26-hAEC-conditioned medium. PKH26-labeled hAEC exosomes were added to the media of KGN cells. (B) The fluorescence signals were detected by confocal microscopy in KGN cells. The nuclei of the hAECs and KGN cells were stained with DAPI (blue) and their cytoskeleton with Actin-Tracker Green (green). Scale bar, 40 (A) and 10 (B) μm. (C) Western blot analyzed the proliferation marker PCNA and the apoptosis-related proteins expression in KGN cells in the different treatment groups. (D) qRT-PCR was used to detect miR-1246, miR-197-5p, miR-1290, miR-4516, miR-4281, and miR-21-5p expression in granulosa cells. (E) The level of miR-1246 and miR-21-5p expression was detected in granulosa cells transfected with miR-1246 and miR-21-5p mimic and inhibitors. (F) Western blot was performed to detect PCNA and cleaved Caspase 3 protein expression in granulosa cells. *$p < 0.05$ versus Control or NC group; #$p < 0.05$ versus the CTX and inhibitor NC group.

contractility.[36] Exosomes help to improve wound management and represent a new therapeutic model for cell-free therapies with decreased side effects for wound repair.[37] A previous study confirmed the superior cardioprotection effect of endometrial mesenchymal stem cells (EnMSCs) relative to that of bone marrow mesenchymal stromal cells (BMMSCs) or adipose-derived mesenchymal stem cells (AdMSCs) and implicated miR-21 as a potential mediator of EnMSC therapy by enhancing cell survival through the PTEN/Akt pathway.[38] Regarding the application of hAEC-derived exosomes in tissue regeneration, some studies have demonstrated that hAEC exosomes accelerates wound healing, inhibits scar formation,[27] restricts lung injury, and enhances endogenous lung repair.[26] In addition, a study showed that proteinase K-pretreated hAEC exosomes accelerate wound healing by promoting the proliferation and migration of fibroblasts, revealing an important role of exosomal miRNAs in wound healing.[39] Research reported that hAEC-derived exosomes carry protein cargo enriched in MAPK signaling pathways, apoptotic and developmental biologic pathways, and exosomal miRNAs mainly enriched in PI3K-Akt, Ras, Hippo, TGF-beta, and focal adhesion pathways.[26] Consistent with this, massive miRNAs were detected in the hAEC-derived exosomes in our study. Importantly, exosomal miRNA-targeted genes were mainly enriched in the PI3K and apoptosis pathways, which were closely related with follicle activation and ovarian function. Because hAEC-derived exosomes contain diverse and numerous miRNAs, it is difficult to determine which miRNA contributes to the repair of ovarian function.

At present, increasing evidence shows that the therapeutic activity of adult stem cells occurs partially through paracrine effects, which give rise to the novel notion of "cell-free" stem cell therapy.[35] A key point related to extracellular vesicles (EVs) or exosome therapy concerns the administration strategy. Research has demonstrated that systemically administered EVs have a short half-life,[40] pointing out the importance of local delivery to avoid rapid clearance and enhance retention in the site of interest.[41] The retention attempt may be clearly reinforced by the choice of biomaterial for embedding stem cell-derived paracrine cytokines or exosomes. Researchers packaged secreted factors from human BMMSCs into poly lactic-*co*-glycolic acid (PLGA) microparticles and then coated them with MSC membranes, and the results demonstrated that these microparticles had regenerative potential in mice with acute myocardial infarction.[42] Furthermore, a synthetic cell-mimicking microparticle (CMMP) carrying secreted proteins could recapitulate stem cell function in tissue repair in a myocardial infarction mouse model.[42,43] The latest research showed that thermoresponsive gel embedding of adipose stem cell-derived EVs promotes esophageal fistula healing in a thermoactuated delivery strategy[44] and integration of stem cell-derived exosomes with *in situ* hydrogel glue as a promising tissue patch for articular cartilage regeneration.[45] In the next study, we will further explore how to combine biomaterials with hAEC-derived exosomes and establish a more effective method for treating POF.

In summary, our findings provided evidence that hAEC-derived exosomes played an effective role in restoring ovarian function in a chemotherapy-induced POF mouse model mainly via transferring the therapeutic effect of microRNAs against apoptosis. The current study uncovered a new therapeutic opportunity and elucidated the underlying molecular mechanism in the process of hAEC-derived exosome-mediated ovarian function recovery.

MATERIALS AND METHODS

Isolation and Culture of hAECs

The isolation and culture of hAECs were conducted as previously described.[15] Human placental tissue was obtained following informed consent from healthy women who tested negative for HIV-I, hepatitis B, and hepatitis C. The acquisition protocol was approved by the Institutional Ethics Committee of the International Peace Maternity and Child Health Hospital (IPMCH). Amniotic membranes were mechanically separated from the chorion, dissected into several segments, and washed with PBS. The membrane segments were incubated for 25 min at 37°C with 0.25% trypsin/EDTA (Gibco, Grand Island, NY, USA). The digested tissue was sequentially filtered through a 40 μm filter and centrifuged at 300 *g* for 5 min at room temperature. Then, the cells were seeded in 100 mm culture dishes containing DMEM/F12 (Gibco, Grand Island, NY, USA) supplemented with 10% fetal bovine serum (FBS; Gibco), 2 mM glutamine, streptomycin (100 μg/mL; Gibco), penicillin (100 U/mL; Gibco), and 10 ng/mL recombinant human epidermal growth factor (EGF; ProSpec). The incubators were set at 37°C and contained 5% CO_2.

Isolation and Identification of hAEC Exosomes

In brief, a total of 5×10^6 hAECs were cultured in a 100 mm culture dish. After 24 h, the complete culture medium was replaced with 10 mL of serum-free DMEM/F12 medium. After another 24 h, the CM from hAECs was collected and centrifuged at 3,000 *g* for 15 min to remove the dead cells and cellular debris. The supernatant was filtered through a 0.22 μm filter (Millipore, Billerica, MA, USA). Then, 10 mL supernatant was further concentrated by centrifugation for 30 min at 10,000 *g* in a pre-rinsed centrifugal filter tube (3 kDa; Amicon Ultra-15; Millipore) to approximately 1 mL. A 1:2 volume of total exosome isolation reagent (Invitrogen, Carlsbad, CA, USA) was added to the concentrated liquid and mixed well by vortexing. After an overnight incubation, the mixture was centrifuged at 10,000 *g* for 60 min to obtain the pellet. The pellet of exosomes was resuspended in PBS. All procedures were performed at 4°C. The exosomes were stored at −80°C or used for the experiments.

The ultrastructure of the exosomes was analyzed under a transmission electron microscope (Zeiss, Oberkochen, Germany). The protein levels of Alix, CD63, and CD9 (representative markers of exosomes) were detected using western blot. To determine the sizes of the purified vesicles, a nanoparticle tracking analysis (NTA) was performed using Zetaview software (Particle Metrix, Meerbusch, Germany).

POF Mouse Model Establishment

Forty-eight wild-type C57BL/6 female mice aged from 7 to 8 weeks were obtained from the Shanghai Experimental Animal Center of the Chinese Academy of Sciences. The mice assigned to the chemotherapy-treated group (Cy, n = 36) received a single intraperitoneal (i.p.) injection of busulfan (Sigma, 30 mg/kg) and CTX (Sigma, 120 mg/kg) to induce the POF model as previously described.[16] The mice in the Sham-control group were injected with an equivalent volume of PBS (Sham, n = 12). PBS, hAEC exosomes, the concentrated hAEC-CM, or hAEC-CM without exosomes (hAECs were pretreated with 10 μM GW4869, a selective inhibitor of N-SMase) was injected into injured ovaries via microinjection needle at 1 (9th, orthotopic injection, a volume of 10 μL) and 2 (10th, tail vein injection, a volume of 100 μL) weeks after chemotherapy. The animals were sacrificed for the subsequent experiments at 10 and 13 weeks, respectively. All animal procedures were approved by the Institutional Animal Care and Use Committee of Shanghai and were performed in accordance with the National Research Council Guide for the Care and Use of Laboratory Animals. Efforts were made to minimize animal suffering and limit the number of animals used in the study.

Histological Analysis

The ovaries were collected at 10 and 13 weeks, fixed in Bouin's solution (containing 5% acetic acid, 9% formaldehyde, and 0.9% picric acid), embedded in paraffin, and serially sectioned at a thickness of 7 μm. H&E staining was used to evaluate the morphological structure of the ovaries, which was observed under light microscopy. The follicle stage was classified according to previously described, accepted definitions.[18] In brief, the blind follicle counts were conducted in every fifth section of the entire ovary by two independent researchers.

The primordial follicle was defined by granulosa cells surrounding a single fusiform oocyte. The primary follicle was surrounded by at least three granulosa cells, resulting in a cubic shape. The secondary follicle appeared to be surrounded by at least two layers of granulosa cells with no follicular cavity. The mature follicles (antral follicles) contained at least two layers of granulosa cells and demonstrated evidence of follicular cavity.

Microarray Analysis

Ovarian tissues from the Sham, PBS, and hAEC-exosome-treated chemotherapy groups were used for microarray profiling. Total RNA was labeled using the Low Input Quick Amp Labeling Kit, and hybridized on the Gene Expression Hybridization Kit. The probes were designed using a microarray (Agilent) and performed by Oe-Biotech (Shanghai, China). The differentially expressed genes among the different groups were determined by KEGG and GO analyses.

Human Granulosa Tumor Cell Line (KGN)

The human ovarian granulosa-like tumor cell line was kindly provided by Dr. Jingjing Xu (IPMCH, School of Medicine, Shanghai Jiao Tong University, Shanghai, China). The KGN cells were cultured in DMEM/F12 (Gibco, Grand Island, NY, USA) supplemented with 10% FBS (Gibco), 2 mM glutamine, streptomycin (100 μg/mL; Gibco), and penicillin (100 U/mL; Gibco). The incubators were set at 37°C and contained 5% CO_2.

hAEC Exosome Uptake Experiment

The hAECs were labeled with a red fluorescent dye (PKH26; Sigma) according to the manufacturer's instructions. Briefly, PKH 26 fluorescent dye was added to the hAEC suspension and incubated for 5 min at room temperature. The reaction was stopped by the addition of an equal volume of exosome-depleted BSA, and the hAECs were washed twice with PBS to remove any unbound dye. Then, the cell-labeled suspension was seeded into a dish. The serum-free medium of PKH26-labeled hAECs was harvested to extract PKH26 exosomes according the method described above. PKH26-hAEC exosomes were added to the medium of the KGN cells, with or without CTX for 24 h. After that, KGN cells and PKH26-labeled hAECs were washed with PBS twice, fixed in 4% paraformaldehyde for 15 min, and washed three times with PBS containing Triton X-100. Actin-Tracker Green (1:100; Beyotime Biotechnology, Shanghai, China) was used for the staining of the cytoskeleton for 60 min at room temperature. After that, the cells were washed with PBS and stained with DAPI (Abcam). The fluorescence signals were captured with a TCS SP5 confocal laser scanning microscope (Leica Microsystems, Wetzlar, Germany).

Western Blot Analysis

The membranes were blocked with 5% milk in TBST (Tris-buffered saline, 10 mM Tris-HCl [pH 7.5], 150 mM NaCl, and 0.1% Tween-20) for 1 hour at room temperature and, incubated with primary antibodies at 4°C overnight. The following primary antibodies and dilutions were used: mouse anti-Alix (1:2,000; CST, Danvers, MA, USA), mouse anti-CD9 (1:500; Santa Cruz, Dallas, TX, USA), mouse anti-CD63 (1:300; Santa Cruz), rabbit anti-Caspase 3 (1:1,000; CST), rabbit anti-phosphorylate PTEN (p-PTEN; 1:1000; CST), rabbit anti-PTEN (1:1,000; CST), rabbit anti-phosphorylate mTOR (p-mTOR, 1:1,000; CST), rabbit anti-mTOR (1:1,000; CST), rabbit anti-phosphorylate Akt (p-Akt, 1:1000; CST), rabbit anti-Akt (1:1,000; CST), rabbit anti-phosphorylate FoxO3a (p-FoxO3a, 1:1,000; CST), rabbit anti-FoxO3a (1:1,000; CST), mouse anti-PCNA (1:1,000; Boster Biological Technology, China), rabbit anti-Bad (1:1000; CST, USA), rabbit anti-Bcl2 (1:1,000; CST, USA), rabbit anti-Bax (1:1,000; CST, USA), and anti-GAPDH (1:5,000; CST). Then, the membranes were incubated with horseradish peroxidase-conjugated secondary antibodies (1:3,000; CST) for 1 hour at room temperature. The visualization of the blots was performed using the standard protocol for electrochemiluminescence (ECL; Santa Cruz Biotechnology, Dallas, TX, USA). The relative intensity of the protein bands was quantified by digital densitometry using ImageJ software (NIH, Bethesda, MD, USA). The level of glyceraldehyde 3-phosphate dehydrogenase (GAPDH) was used as an internal standard.

Double-Fluorescence Immunolabeling

To detect the double-fluorescence signals of CD34 and EdU, the sections were incubated with a primary rabbit monoclonal anti-CD34 antibody (1:1,000; Abcam, Cambridge, MA, USA) overnight at 4°C. After they were washed three times with PBS, the sections were incubated with a 1:200 dilution of anti-rabbit IgG rhodamine (Santa Cruz) for 1 hour at 37°C. After another washing with PBS, the sections were labeled with Apollo and Hoechst staining (EdU staining kit; Ruibo, China), as per the instructions. After another wash with PBS, the sections were coverslipped with fluorescence mounting medium. The fluorescence signals could be directly detected at an excitation of 488 nm and emission of 525 nm.

Apoptosis Assay

To detect apoptosis in ovarian sections, TUNEL staining kits (Roche Applied Science, USA) were used according to the manufacturer's instructions. The nuclei were counterstained using DAPI (Abcam, USA). The images were captured under a fluorescence microscope.

RNA Extraction and qRT-PCR

The ovaries were collected in TRIzol reagent (Invitrogen, Carlsbad, CA, USA), and the total RNA was extracted according to the manufacturer's instructions. A total of 1 μg RNA was converted to cDNA with a Takara kit (Applied Biosystems Foster City, CA, USA; Takara, Shiga, Japan). The genes of interest were amplified with a 7900HT fast real-time PCR system (Applied Biosystems) and a SYBR Green Real-time PCR Master Mix (Applied Biosystems/Takara). The PCR primers were designed according to the cDNA sequences in the NCBI database. The following primer sequences were used: *HAS2*: forward, 5′-AAGACCCTATGGTTGGAGGTGTT-3′, reverse, 5′-CA TTCCCAGAGGACCGCTTAT-3′; *PTX3*: forward, 5′GGACAAC GAAATAG ACAATGGACTT-3′, reverse, 5′-CGAGTTCTCCAG CATGATGAAC-3′; and *GAPDH*: forward, 5′-CCAATGTGTCCG TCGTGGATCT-3′, reverse, 5′-GTTGAAGTCGCAGGAGACAA CC-3′. The cycling conditions used for the PCR analysis were as

follows: 95°C for 5 s, 60°C for 30 s, and 72°C for 30 s (40 cycles). Mouse-GAPDH was used as an internal control. The $2^{-\Delta\Delta Ct}$ method was employed to determine the relative mRNA expression level.

A total of 1 μg RNA of KGN and hAEC exosomes was extracted and converted to cDNA using a miScript RTKit (QIAGEN, Hilden, Germany). The SYBR green method was used to detect the expression of the miRNAs. qRT-PCR results were recorded as cycle threshold (Ct) numbers and, normalized against the internal control (hsa-U6 and cel-miR-39). The $2^{-\Delta\Delta Ct}$ method was employed to determine the relative miRNA expression levels.

MicroRNA Analysis in hAEC-Derived Exosomes

The total RNA was extracted from five hAEC exosomes (hAEC exosomes 1, 2, 3, 4, and 5, obtained from five healthy donors), and the microRNA expression profile was analyzed with a NanoString platform according to the manufacturer's instructions. Human microRNA microarray (Shanghai Bohao Biotechnology, Shanghai, China) was used for detecting miRNA in hAEC exosomes. nSolver was used to normalize the number of reads of each miRNA to the positive controls and the top 100 reads. Negative controls were used as a threshold for the background subtraction.

KGN Cells Transfection

KGN cells were transfected with miR-1246 and miR-21-5p mimics, inhibitors, and control (GenePharma, China) using Lipofectamine RNAi MAX Reagent (Invitrogen, USA). After 24 h of transfection, the cells were collected for qRT-PCR and western blot analysis.

Statistical Analysis

The mean and SEM of the experimental variables were calculated. The statistical significance was calculated using GraphPad Prism (GraphPad Software, San Diego, CA). The western blot, qRT-PCR, and follicle count data were analyzed using two-way ANOVA with the least-significant difference (LSD) test. Confidence intervals of 95% were deemed statistically significant. The differences between the groups were considered significant at $p < 0.05$.

AUTHOR CONTRIBUTIONS

Q.Z. and J.S. carried out the animal model establishment, immunohistochemistry, and molecular analysis. Y.H., S.B., and C.W. carried out the cell culture, flow cytometry, and western blot. Y.G. and T.G. participated in follicle counting. Q.Z., J.S., and B.L. participated in the data analysis. Q.Z. and D.L. conceived and designed the study and drafted the manuscript. All authors read and approved the final manuscript.

CONFLICTS OF INTEREST

The authors declare no competing interests.

ACKNOWLEDGMENTS

This study was funded by the National Key Research and Developmental Program of China (2018YFC1004800 and 2018YFC1004802), Shanghai Municipal Education Commission-Gaofeng Clinical Medicine Grant Support (20152236), Shanghai Municipal Health Bureau, Shanghai, China (20144Y0048), the National Natural Science Foundation of China (81701397 and 81741013), the Opening Fund of Key Laboratory of the Diagnosis and Treatment Research of Reproductive Disorders of Zhejiang Province (2018001), and the Interdisciplinary Program of Shanghai Jiao Tong University (YG2014QN12 and YG2015ZD11).

REFERENCES

1. Podfigurna-Stopa, A., Czyzyk, A., Grymowicz, M., Smolarczyk, R., Katulski, K., Czajkowski, K., and Meczekalski, B. (2016). Premature ovarian insufficiency: the context of long-term effects. J. Endocrinol. Invest. *39*, 983–990.
2. Jankowska, K. (2017). Premature ovarian failure. Przegl. Menopauz. *16*, 51–56.
3. Adhikari, D., and Liu, K. (2009). Molecular mechanisms underlying the activation of mammalian primordial follicles. Endocr. Rev. *30*, 438–464.
4. Kalich-Philosoph, L., Roness, H., Carmely, A., Fishel-Bartal, M., Ligumsky, H., Paglin, S., Wolf, I., Kanety, H., Sredni, B., and Meirow, D. (2013). Cyclophosphamide triggers follicle activation and "burnout"; AS101 prevents follicle loss and preserves fertility. Sci. Transl. Med. *5*, 185ra62.
5. Sheikhansari, G., Aghebati-Maleki, L., Nouri, M., Jadidi-Niaragh, F., and Yousefi, M. (2018). Current approaches for the treatment of premature ovarian failure with stem cell therapy. Biomed. Pharmacother. *102*, 254–262.
6. Ding, L., Yan, G., Wang, B., Xu, L., Gu, Y., Ru, T., Cui, X., Lei, L., Liu, J., Sheng, X., et al. (2018). Transplantation of UC-MSCs on collagen scaffold activates follicles in dormant ovaries of POF patients with long history of infertility. Sci. China Life Sci. *61*, 1554–1565.
7. Chen, L., Guo, S., Wei, C., Li, H., Wang, H., and Xu, Y. (2018). Effect of stem cell transplantation of premature ovarian failure in animal models and patients: A meta-analysis and case report. Exp. Ther. Med. *15*, 4105–4118.
8. Herraiz, S., Buigues, A., Díaz-García, C., Romeu, M., Martínez, S., Gómez-Seguí, I., Simón, C., Hsueh, A.J., and Pellicer, A. (2018). Fertility rescue and ovarian follicle growth promotion by bone marrow stem cell infusion. Fertil. Steril. *109*, 908–918.e2.
9. Li, J., Yu, Q., Huang, H., Deng, W., Cao, X., Adu-Frimpong, M., Yu, J., and Xu, X. (2018). Human chorionic plate-derived mesenchymal stem cells transplantation restores ovarian function in a chemotherapy-induced mouse model of premature ovarian failure. Stem Cell Res. Ther. *9*, 81.
10. Di Germanio, C., Bernier, M., de Cabo, R., and Barboni, B. (2016). Amniotic Epithelial Cells: A New Tool to Combat Aging and Age-Related Diseases? Front. Cell Dev. Biol. *4*, 135.
11. Zhu, D., Tan, J., Maleken, A.S., Muljadi, R., Chan, S.T., Lau, S.N., Elgass, K., Leaw, B., Mockler, J., Chambers, D., et al. (2017). Human amnion cells reverse acute and chronic pulmonary damage in experimental neonatal lung injury. Stem Cell Res. Ther. *8*, 257.
12. Evans, M.A., Lim, R., Kim, H.A., Chu, H.X., Gardiner-Mann, C.V., Taylor, K.W.E., Chan, C.T., Brait, V.H., Lee, S., Dinh, Q.N., et al. (2018). Acute or Delayed Systemic Administration of Human Amnion Epithelial Cells Improves Outcomes in Experimental Stroke. Stroke *49*, 700–709.
13. Yawno, T., Sabaretnam, T., Li, J., McDonald, C., Lim, R., Jenkin, G., Wallace, E.M., and Miller, S.L. (2017). Human Amnion Epithelial Cells Protect Against White Matter Brain Injury After Repeated Endotoxin Exposure in the Preterm Ovine Fetus. Cell Transplant. *26*, 541–553.
14. Lim, R., Hodge, A., Moore, G., Wallace, E.M., and Sievert, W. (2017). A Pilot Study Evaluating the Safety of Intravenously Administered Human Amnion Epithelial Cells for the Treatment of Hepatic Fibrosis. Front. Pharmacol. *8*, 549.
15. Wang, F., Wang, L., Yao, X., Lai, D., and Guo, L. (2013). Human amniotic epithelial cells can differentiate into granulosa cells and restore folliculogenesis in a mouse model of chemotherapy-induced premature ovarian failure. Stem Cell Res. Ther. *4*, 124.
16. Zhang, Q., Xu, M., Yao, X., Li, T., Wang, Q., and Lai, D. (2015). Human amniotic epithelial cells inhibit granulosa cell apoptosis induced by chemotherapy and restore the fertility. Stem Cell Res. Ther. *6*, 152.

17. Yao, X., Guo, Y., Wang, Q., Xu, M., Zhang, Q., Li, T., and Lai, D. (2016). The Paracrine Effect of Transplanted Human Amniotic Epithelial Cells on Ovarian Function Improvement in a Mouse Model of Chemotherapy-Induced Primary Ovarian Insufficiency. Stem Cells Int. *2016*, 4148923.

18. Zhang, Q., Bu, S., Sun, J., Xu, M., Yao, X., He, K., and Lai, D. (2017). Paracrine effects of human amniotic epithelial cells protect against chemotherapy-induced ovarian damage. Stem Cell Res. Ther. *8*, 270.

19. Leaw, B., Zhu, D., Tan, J., Muljadi, R., Saad, M.I., Mockler, J.C., Wallace, E.M., Lim, R., and Tolcos, M. (2017). Human amnion epithelial cells rescue cell death via immunomodulation of microglia in a mouse model of perinatal brain injury. Stem Cell Res. Ther. *8*, 46.

20. Hodge, A., Lourensz, D., Vaghjiani, V., Nguyen, H., Tchongue, J., Wang, B., Murthi, P., Sievert, W., and Manuelpillai, U. (2014). Soluble factors derived from human amniotic epithelial cells suppress collagen production in human hepatic stellate cells. Cytotherapy *16*, 1132–1144.

21. Keerthikumar, S., Chisanga, D., Ariyaratne, D., Al Saffar, H., Anand, S., Zhao, K., Samuel, M., Pathan, M., Jois, M., Chilamkurti, N., et al. (2016). ExoCarta: A Web-Based Compendium of Exosomal Cargo. J. Mol. Biol. *428*, 688–692.

22. Skotland, T., Sandvig, K., and Llorente, A. (2017). Lipids in exosomes: Current knowledge and the way forward. Prog. Lipid Res. *66*, 30–41.

23. Jiang, N., Xiang, L., He, L., Yang, G., Zheng, J., Wang, C., Zhang, Y., Wang, S., Zhou, Y., Sheu, T.J., et al. (2017). Exosomes Mediate Epithelium-Mesenchyme Crosstalk in Organ Development. ACS Nano *11*, 7736–7746.

24. Singla, D.K. (2016). Stem cells and exosomes in cardiac repair. Curr. Opin. Pharmacol. *27*, 19–23.

25. Basu, J., and Ludlow, J.W. (2016). Exosomes for repair, regeneration and rejuvenation. Expert Opin. Biol. Ther. *16*, 489–506.

26. Tan, J.L., Lau, S.N., Leaw, B., Nguyen, H.P.T., Salamonsen, L.A., Saad, M.I., Chan, S.T., Zhu, D., Krause, M., Kim, C., et al. (2018). Amnion Epithelial Cell-Derived Exosomes Restrict Lung Injury and Enhance Endogenous Lung Repair. Stem Cells Transl. Med. *7*, 180–196.

27. Zhao, B., Zhang, Y., Han, S., Zhang, W., Zhou, Q., Guan, H., Liu, J., Shi, J., Su, L., and Hu, D. (2017). Exosomes derived from human amniotic epithelial cells accelerate wound healing and inhibit scar formation. J. Mol. Histol. *48*, 121–132.

28. Fu, X., He, Y., Wang, X., Peng, D., Chen, X., Li, X., and Wang, Q. (2017). Overexpression of miR-21 in stem cells improves ovarian structure and function in rats with chemotherapy-induced ovarian damage by targeting PDCD4 and PTEN to inhibit granulosa cell apoptosis. Stem Cell Res. Ther. *8*, 187.

29. Cui, Y., Miyoshi, K., Claudio, E., Siebenlist, U.K., Gonzalez, F.J., Flaws, J., Wagner, K.U., and Hennighausen, L. (2002). Loss of the peroxisome proliferation-activated receptor gamma (PPARgamma) does not affect mammary development and propensity for tumor formation but leads to reduced fertility. J. Biol. Chem. *277*, 17830–17835.

30. Chen, X.Y., Xia, H.X., Guan, H.Y., Li, B., and Zhang, W. (2016). Follicle Loss and Apoptosis in Cyclophosphamide-Treated Mice: What's the Matter? Int. J. Mol. Sci. *17*, E836.

31. Ernst, E.H., Grøndahl, M.L., Grund, S., Hardy, K., Heuck, A., Sunde, L., Franks, S., Andersen, C.Y., Villesen, P., and Lykke-Hartmann, K. (2017). Dormancy and activation of human oocytes from primordial and primary follicles: molecular clues to oocyte regulation. Hum. Reprod. *32*, 1684–1700.

32. Roness, H., Kashi, O., and Meirow, D. (2016). Prevention of chemotherapy-induced ovarian damage. Fertil. Steril. *105*, 20–29.

33. Jang, H., Lee, O.H., Lee, Y., Yoon, H., Chang, E.M., Park, M., Lee, J.W., Hong, K., Kim, J.O., Kim, N.K., et al. (2016). Melatonin prevents cisplatin-induced primordial follicle loss via suppression of PTEN/AKT/FOXO3a pathway activation in the mouse ovary. J. Pineal Res. *60*, 336–347.

34. Zhou, L., Xie, Y., Li, S., Liang, Y., Qiu, Q., Lin, H., and Zhang, Q. (2017). Rapamycin Prevents cyclophosphamide-induced Over-activation of Primordial Follicle pool through PI3K/Akt/mTOR Signaling Pathway in vivo. J. Ovarian Res. *10*, 56.

35. Maguire, G. (2013). Stem cell therapy without the cells. Commun. Integr. Biol. *6*, e26631.

36. Mayourian, J., Ceholski, D.K., Gorski, P., Mathiyalagan, P., Murphy, J.F., Salazar, S.I., Stillitano, F., Hare, J.M., Sahoo, S., Hajjar, R.J., et al. (2018). Exosomal microRNA-21-5p Mediates Mesenchymal Stem Cell Paracrine Effects on Human Cardiac Tissue Contractility. Circ. Res. *122*, 933–944.

37. Golchin, A., Hosseinzadeh, S., and Ardeshirylajimi, A. (2018). The exosomes released from different cell types and their effects in wound healing. J. Cell. Biochem. *119*, 5043–5052.

38. Wang, K., Jiang, Z., Webster, K.A., Chen, J., Hu, H., Zhou, Y., Zhao, J., Wang, L., Wang, Y., Zhong, Z., et al. (2017). Enhanced Cardioprotection by Human Endometrium Mesenchymal Stem Cells Driven by Exosomal MicroRNA-21. Stem Cells Transl. Med. *6*, 209–222.

39. Zhao, B., Li, X., Shi, X., Shi, X., Zhang, W., Wu, G., Wang, X., Su, L., and Hu, D. (2018). Exosomal MicroRNAs Derived from Human Amniotic Epithelial Cells Accelerate Wound Healing by Promoting the Proliferation and Migration of Fibroblasts. Stem Cells Int. *2018*, 5420463.

40. Vader, P., Mol, E.A., Pasterkamp, G., and Schiffelers, R.M. (2016). Extracellular vesicles for drug delivery. Adv. Drug Deliv. Rev. *106* (Pt A), 148–156.

41. György, B., Hung, M.E., Breakefield, X.O., and Leonard, J.N. (2015). Therapeutic applications of extracellular vesicles: clinical promise and open questions. Annu. Rev. Pharmacol. Toxicol. *55*, 439–464.

42. Luo, L., Tang, J., Nishi, K., Yan, C., Dinh, P.U., Cores, J., Kudo, T., Zhang, J., Li, T.S., and Cheng, K. (2017). Fabrication of Synthetic Mesenchymal Stem Cells for the Treatment of Acute Myocardial Infarction in Mice. Circ. Res. *120*, 1768–1775.

43. Tang, J., Shen, D., Caranasos, T.G., Wang, Z., Vandergriff, A.C., Allen, T.A., Hensley, M.T., Dinh, P.U., Cores, J., Li, T.S., et al. (2017). Therapeutic microparticles functionalized with biomimetic cardiac stem cell membranes and secretome. Nat. Commun. *8*, 13724.

44. Silva, A.K.A., Perretta, S., Perrod, G., Pidial, L., Lindner, V., Carn, F., Lemieux, S., Alloyeau, D., Boucenna, I., Menasché, P., et al. (2018). Thermoresponsive Gel Embedding Adipose Stem Cell-Derived Extracellular Vesicles Promotes Esophageal Fistula Healing in a Thermo-Actuated Delivery Strategy. ACS Nano. *12*, 9800–9814.

45. Liu, X., Yang, Y., Li, Y., Niu, X., Zhao, B., Wang, Y., Bao, C., Xie, Z., Lin, Q., and Zhu, L. (2017). Integration of stem cell-derived exosomes with in situ hydrogel glue as a promising tissue patch for articular cartilage regeneration. Nanoscale *9*, 4430–4438.